Skeletal morphology of the holotype of *Gymnallabes nops* Roberts & Stewart, 1976, using micro CT-scanning

by

Stijn DEVAERE (1), Dominique ADRIAENS (1), Guy G. TEUGELS† (2),
Nora M. DE CLERCK (3) & Andrei A. POSTNOV (3, 4)

ABSTRACT. - One of the major problems in the anguilliform Clariidae is the taxonomical validity and the systematic position of *Gymnallabes nops*. This vagueness is largely due to the fact that the description of this species is based on the holotype only, and no additional specimens are known. This also means that past studies on this holotype were limited to non-invasive research, such as external morphology and X-rays. These methods, however, yield only a limited number of valuable characters. In this study a high-resolution desktop X-ray microtomography instrument (CT-scan) was used. This enables us to confirm the results of the radiographies but also to perform a detailed osteological study, without damaging the holotype. The osteological survey showed similarities with other anguilliform clariids, in particular with *Platyallabes tihoni* and *Gymnallabes typus*. Besides these traits, *G. nops* shows a set of characters, revealed in this study, unique among the clariids, such as a reduction of the infraorbital bones in number and size, a large anterior outgrowth of the opercle, a clearly visible epiphyseal bridge and the typical positioning of entopterygoid and metapterygoid bones. These extra results may help to clarify the validity and the phylogenetic position of *G. nops*.

RÉSUMÉ. - Morphologie squelettique de l'holotype de *Gymnallabes nops* Roberts & Stewart, 1976, étudiée par tomodensitométrie à haute résolution.

Un des plus grands problèmes chez les Clariidae anguilliformes est la validité taxinomique et la position systématique de *Gymnallabes nops*. Cette situation est largement due au fait que la description de cette espèce n'est fondée que sur l'holotype. Cela signifie également que les études réalisées sur celui-ci sont limitées aux études non invasives, comme la morphologie extérieure et l'usage des radiographies. Ces méthodes ne produisent que des données valables mais limitées. Dans cette étude, un scanner rayons X à haute résolution (CT-scan) a été utilisé, permettant de confirmer les résultats des radiographies, mais aussi d'accomplir une étude ostéologique détaillée, sans abîmer l'holotype. Cette étude ostéologique montre les similarités existant avec d'autres Clariidae anguilliformes, en particulier avec *Platyallabes tihoni* et *Gymnallabes typus*. En plus de ces caractères, *Gymnallabes nops* montre un ensemble de caractères uniques, comme par exemple une réduction de la taille et du nombre des osselets infraorbitaires, un operculaire avec une grande expansion antérieure, un pont épiphysaire non couvert par les plaques frontales et la mise en place typique des osselets entoptérygoïde et métaptérygoïde. Ces résultats supplémentaires peuvent aider à clarifier la validité et la position phylogénétiques de cette espèce.

Key words. - Siluriformes - Clariidae - *Gymnallabes nops* - Holotype - skeleton - X-ray scanning.

The freshwater Clariidae is one of the 37 catfish families known within the Siluriformes order (Sabaj *et al*., 2004). Their diversity is the largest on the African continent. Besides in Africa, they can also be found in Syria, southern Turkey and some parts of Southeast Asia (Teugels, 2003). Although, some of the more generalized, fusiform species, in particular *Clarias gariepinus* (Burchell, 1922), show a large distribution, the occupation of the anguilliform species is a more specialized, burrowing niche (Adriaens *et al*., 2001). They occur only in Equatorial Central and West Africa (Boulenger, 1911; Poll, 1957; Teugels *et al*., 1990; Teugels, 2003).

Clariid catfishes are characterized by an elongate body, long dorsal and anal fins, the presence of four pairs of bar-bels, and especially by the unique presence of a supra-branchial organ, formed by arborescent structures from the second and fourth gill arches (Greenwood, 1961; Teugels and Adriaens, 2003).

The anatomy of the anguilliform clariids is poorly known. Only a few studies have superficially described the cranial morphology into detail (Poll, 1957, 1977; Cabuy *et al*., 1999; Devaere *et al*., 2001). This is certainly the case for *Gymnallabes nops*, on which, to this moment, no morphological research has been done. The fact that the holotype is the only found representative of *G. nops* can be considered as the main reason for this deficiency, as this allows only a narrow field of non-invasive studies that can be performed on such unique material. Thanks to the use of computerized

---

(1) Ghent University, Evolutionary Morphology of Vertebrates, K.L. Ledeganckstraat 35, B-9000 Ghent, BELGIUM. [stijn.devaere@ugent.be]

(2) Africa Museum, Ichthyology Department, B-3080 Tervuren, BELGIUM and KULeuven, Section for Ecology and Systematics, B-3000 Leuven, BELGIUM.

(3) University of Antwerp (RUCA), Microtomography, Department of Biomedical Sciences, Groenerborgerlaan 171, B-2018 Antwerpen, BELGIUM.

(4) University of Antwerp (RUCA), Department of Physics, Groenerborgerlaan 171, B-2018 Antwerpen, BELGIUM.

microtomography (mCT), we obtained 3D information of the complete skeleton in a non-destructive manner. The objectives of this paper are therefore: (1) to give a detailed description of the cranium and the most relevant post-cranial structures; (2) to use this new information for the comparison with other anguilliform clariids; (3) to describe *G. nops* based on characters, found in this study and (4) to provide diagnostic characters for this species.

MATERIALS AND METHODS

Material examined

The holotype of *Gymnallabes nops* Roberts & Stewart, 1976 (MCZ 50.298) (Fig. 1) was obtained from the Museum of comparative Zoology, Harvard University (MCZ). The specimen was collected in Tadi, the lower Congo-River basin (5°14'S, 13°56'E). The sample site is a 2 m deep, backwater with boulders, with a silty or sandy bottom (Roberts and Stewart, 1976).

Comparative material examined

Museum abbreviations are listed in Leviton *et al.* (1985).

Channallabes apus. - Angola: Ambriz, BMNH 1873.7.28.16 (holotype). Dem. Rep. Congo: Bokalakala, MRAC 175247-270, 10 ex.; Kinshasa, MRAC 97-056-P-0001-0003, 2 ex.; Bumba, MRAC 88-25-P-2192-227, 36 ex.; Boma, MRAC 939, 1 ex.; Riv. Lula, Bushimaie, MRAC 1535051 ex.; Kelé, MRAC 1491, 1 ex.; Stanleyville, MRAC 30893-30900, 8 ex., MRAC 88-01-P-1976-1992, 17 ex.; Riv. Ruki, Eala, MRAC 14747-49, 3 ex.; Lake Tumba swamp area, MRAC 46299, 1 ex.; Katanga, MRAC 39480, 1 ex.; Riv. Botota, Keseki, MRAC 67763-77, 15 ex.; Mwilambongo, MRAC 72886-887, 2 ex.; Dekese, Riv. Lofu, Anga, MRAC 153352, 1 ex.; Yangambi, MRAC 68700,1 ex.; Riv. Oubangui, Imfondo, MNHN 1922-0029,1 ex.; Loango, MNHN 1924-0079, 1 ex.; MNHN 1924-0080, 1 ex.; Sangha, MNHN 1925-0137, 1 ex.; Mogende, MNHN 1926-0155-59, 5 ex.; Riv Congo, MNHN, 1937-0124-25, 1 ex.; Stanleypool, Bamu, MNHN 1958-0111, 1 ex.; Boloko, Riv. Likouala, MNHN 1962-0401, 7 ex.; Mossaka, Riv. Likouala, MNHN 1963-0402, 2 ex.; Riv. Loadjili, Songolo, MNHN 1967-0143, 6 ex.; Mangala, BMNH 1896.3.9.17, 1 ex.; Riv. Lebuzi, Kaka Muno, BMNH 1912.4.1411-12, 2 ex.; Lower Congo, BMNH 1887.1.13.8-9, 2 ex.; Stanley Falls, BMNH 1889.11.20.5, 1 ex.; New Antwerp, Upper Congo, BMNH 1899.2.20.16, 1 ex.; Siala-Ntoto Swamps, BMNH 99.11.27.92, 1 ex.; Bangyville, Ubangi, BMNH 1907.12.26.34, 1 ex.; Kashi, Lulua, MHNG 1248.3, 1 ex.; Banana, NMW 47240-42; Mollunda, NMW 47245, 4 ex., NMW 47246, 1 ex. Congo: Yangala Youbi, MNHN 1967-0146, 1 ex.; Djembo, Kouilou, MNHN 1967-0147, 1 ex.; Cayo, MNHN 1989-0527, 1 ex.; Riv. Nanga, between Boukou-Zassi and Kouilou swamp area, MRAC 90-57-P2315, 1 ex.; Sintou, Riv. Kibombo, Kouilou, MNHN 1967-0144, 1 ex.; Riv. Loadjili, Songolo, Pointe Noire, MNHN 1967-0145, 6 ex.; Angola: Caungula, Mabete, Riv. Uamba, MRAC 162088, 1 ex.; Riv. Camuconda, Tchimenji, MRAC 162089, 162090-094, 5 ex., 162095-100, 6 ex.; Riv Ganga-Ludchimo, MRAC162083-086, 4 ex.

Dolichallabes microphthalmus. - Dem. Rep. Congo: Kunungu, MRAC 44655, adult male, 229 mm SL (holotype), MRAC 44656-659, 3 ex. (196-210 mm SL) and 62407, 1 ex., 188 mm SL (paratypes), MRAC 57662, 1 ex., 196 mm SL, MRAC 18850, 1 ex., 90 mm SL; Boende swamps, MRAC 101843, 1 ex., 149 mm SL, 176123-124, 1 ex., 68 mm SL; Bokuma, MRAC 79093, 1 ex., 134 mm SL, 93774, 1 ex., 66 mm SL; Bokuma - Tchuapa, MRAC 79258-260, 3 ex. (85-126 mm SL); Ndwa (Boloko), MRAC 78808-810, 3 ex. (99-110 mm SL); Inonge, MRAC 96672, 1 ex., 110 mm SL; Maylimbe, Tshela, MRAC 66721, 1 ex., 97 mm SL.

Gymnallabes alvarezi. - Rep. Congo: Zanaga, Lésala, MRAC 8-22-P-1047-050, 1 ex., 141 mm SL.

Gymnallabes typus. - Nigeria: Old Calabar, BMNH 1866.12.4, 2 ex. (Syntypes); Umu-Eze Amambra, MRAC 84-16-P-1-2, 1 ex.; Riv. Sombreiro, East of Erema, MRAC 91-067-P0134, 1 ex.; Niger Delta, MRAC 97-030-P-0001-0010, 10 ex.; lake Odediginni, Agudama, Yenagoa, MRAC 92-083-P-0035-0036, 1 ex.; Okaka, Epie Creek, Between Nun an Rashi Riv, MRAC 97-085-P-0001-0004, 4 ex.; Riv. Sombreiro, Odiemerenyi, Ahoada, MRAC 91-067-P-0135-0136, 1 ex.; New Calabar, Choba, MRAC 91-105-P-1, 1 ex.; Rumuji Swamps, MRAC 86-10-P-72, 1 ex.; Oshika, MRAC 84-28-P-28, 1 ex., MRAC 84-28-P-25, 1 ex.; Riv. Cron, Itu, MRAC 88-36-P-10, 1 ex.; Between Sapele and War, Niger Delta, MRAC 74-29-P-600, 1 ex.; Muoha, New Calabar, MRAC 91-10-P-478, 1 ex.; Biseni, Taylor Creek, MRAC 91-01-P278, 1 ex.; Ossomari, BMNH 1902.11.10.119, 1 ex. Cameroun: Riv. Kom, Ntem, Aboulou, MRAC 73-18-P-3307-309, 1 ex.

Platyclarias machadoi. - Angola: Cuango, Cafunfo, Riv. Borio, MRAC 78-6-P-1345, adult female, 181 mm SL (holotype), 78-6-P-1346-1367, 21 ex., (76.0-146 mm SL).

Platyallabes tihoni. - Dem. Rep. Congo: Kingabwa, Stanley pool, MRAC 13307 (Holotype); Kinsuka, MRAC 73-68-P-143, 1 ex., 138698-699, 2 ex., 125345-349, 4 ex., 73-22-P-3127, 3 ex.;
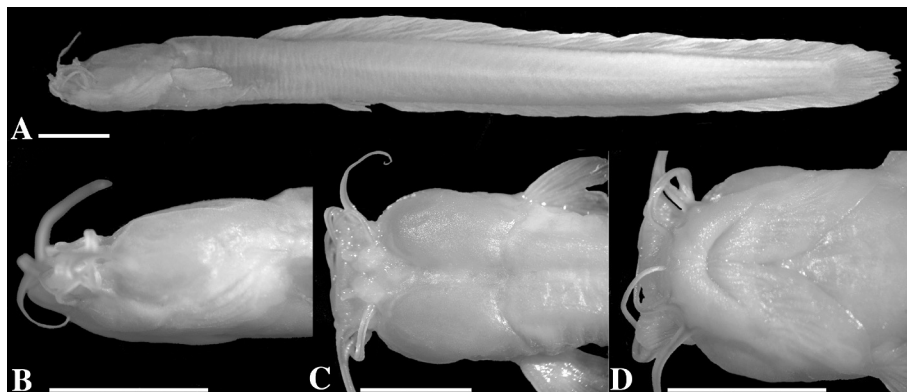

Figure 1. - **A**: Holotype of *Gymnallabes nops* (56.57 mm SL) (MCZ 50298); **B**: Lateral side; **C**: Dorsal side; **D**: Ventral side of head. (Scale bars = 5 mm). (Photos: S. Devaere). *[A : Holotype de* Gymnallabes nops *; B : Vue latérale ; C : Vue dorsale ; D : Vue ventrale de la tête. (Échelles = 5 mm). (Photos : S. Devaere).]*

Bulu, Luozi, BMNH 1976.5.21.30-39, 9 ex., MCZ 50239, 13 ex.; Inga, 88947, 50537, 15 ex.; Tadi, Kibunzi, MCZ 50297, 5 ex.

Measurements

All measurements were made on the holotype using a high-resolution desktop X-ray microtomography instrument [Skyscan-1072, Belgium (www.skyscan.be)]. A Tungsten air-cooled micro-focus X-rays tube with 9-μm spot size and a maximum voltage of 80 kV was used as a source. A 12-bit 1 mega-pixel low-noise CCD camera was applied as a detector. During acquisition both the X-ray source and the camera remained motionless while the object was rotated around its vertical axis. The system allows achieving 9-micron resolution but measured resolution depends on the size of the object and on the contrast. Biggest field of view possible for this device was 20 mm. The investigated specimen was too big for one acquisition so it was scanned 5 times and then reconstructed separately and assembled in one model afterwards. As our fish was fixated for a time in a decalcifying medium, the observed contrast was much lower than for ordinary fresh fish bones. That constrained us to use lower energies to improve contrast for soft tissues. The sample was scanned with 40 kV X-ray tube voltage, 0.9-degree rotation step and approximately 10 sec exposure time per individual shadow projection. After the shadow images were collected they were reconstructed into virtual cross-section using Feldkamp cone-beam algorithm. These cross-sections are the analogues of histological slices. The advantage is that the specimen remained intact although the resolution is lower than in classical histology. Another important advantage is that micro-tomography provides isotropic resolution thus allowing to build 3D-models (see following illustrations). 3D models presented in this paper were created with ANT software supplied by Skyscan with the instrument. (ANT software, Skyscan, Belgium) (Postnov *et al.*, 2002; De Clerck *et al.*, 2003).

Furthermore, a set of 33 metric measurements were taken point-to-point using digital callipers to 0.1 mm (Digital ruler, Mauser), interfaced directly with a computer. Measurements terminology follows that of Devaere *et al.* (2004): total length (TL); standard length (SL); preanal length (PaL); anal fin length (AFL); dorsal fin length (DFL); prepelvic length (PPvL); prepectoral length (PPcL); predorsal length (PdL); distance between the occipital process and the dorsal fin (SPDFL); pelvic fin length (PvFL), pectoral fin length (PcFL); pectoral spine length (PcSL); caudal peduncle depth (CPD); body depth at anus (ABD); maxillary barbel length (MxB); external mandibular barbel length (EmnB); internal mandibular barbel length (ImnB); nasal barbel length (NB); interpelvic distance (IpvD); interpectoral distance (IpcD); skull length (SkL); postorbital length (PoL); skull width (SkW); supraoccipital process length (SpL); supraoccipital process width (SpW); interorbital distance (IoD); anterior

nostril interdistance (ANID); posterior nostril interdistance (PNID); rostral skull width (RSkW); orbital skull width (OskW); skull height (SkH); eye diameter (ED); snout height (SnH); prehyoid length (PhL); internal mandibular interdistance (ImnID); external mandibular interdistance (EmnID); mouth width (MW) and skull roof width (SkR). The following meristic counts were made, using the radiographies made with a Bennett X-ray (25-50kV, 25-150 Ma, 1/30-20 sec, focus distance: 0.3-0.6 m): total number of vertebrae (TV), number of ribs (RB).

We compared the holotype with a large sample of four other anguilliform species; *Platyallabes tihoni* (Poll, 1944), *Gymnallabes typus* Günther, 1867, *Dolichallabes microphthalmus* Poll, 1942, *Channallabes apus* (Günther, 1873) and *Platyclarias machadoi* Poll, 1977.

Analyses

The morphometric data and the meristic counts were submitted to a Principle Component Analysis (Bookstein *et al.*, 1985). Morphometric data were log-transformed, so that the non-normality effects could be minimized before the PCA was run on the covariance matrix. The first principle component was not used since it is considered as a size factor, the other components as shape factors, independent of size (Teugels *et al.*, 1999). Different combinations of components were used to give the plot that expressed the most variation.

RESULTS

Neurocranium

Ethmoid region. - The nasal bone (Figs 2, 3), covering the nasal sac and enclosing the anterior-most part of the supraorbital canal, is reduced to a partially open, elongated bone, with little to no lateral plate extensions present. The supraorbital canal appears to split in this bone, as a lateral pore can be distinguished.

The mesethmoid (Figs 2, 3A) shows a substantial constriction caudally from the two rostral wings. It is sutured to the frontals, by means of large interdigitations. The main part of the lateral ethmoid is covered by the frontal. Ventrally, the mesethmoid supports the premaxillary bones. Although very restricted, the mesethmoid makes contact with the anterior fontanel. The lateral ethmoid shows a long, pointed lateral process (Figs 2, 3). Anteriorly, the supraorbital canal leaves the neurocranium where the mesethmoid and lateral ethmoid suture. At this point the supraorbital canal is covered by the rostral extension of the frontal. Since there is no second infraorbital bone (see below), the lateral ethmoid shows only an articulation surface for the autopalatine. The arrow-shaped prevomer interconnects with the
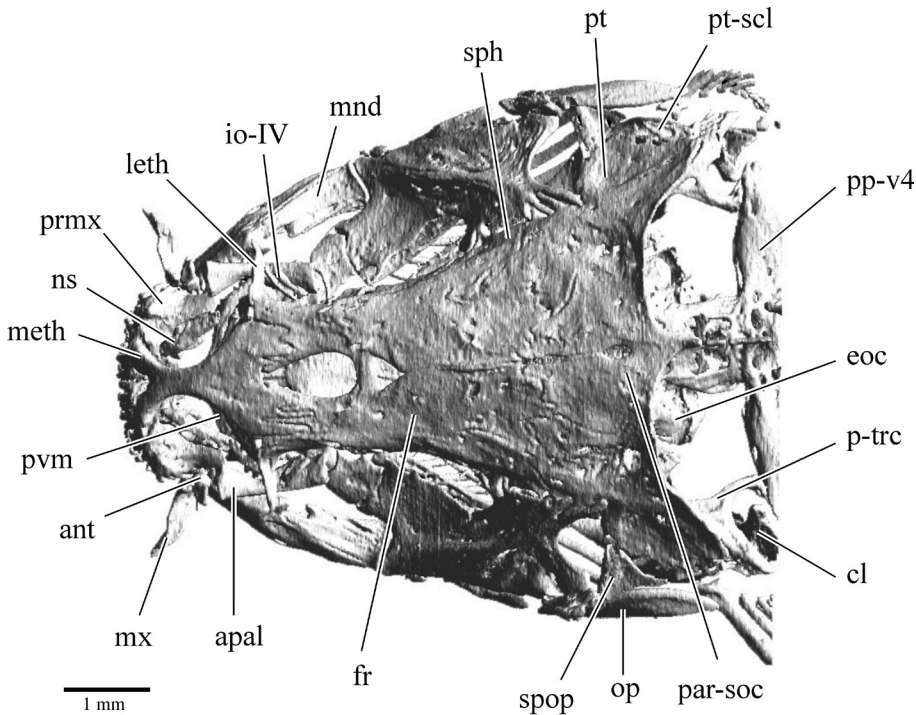
Figure 2. - Dorsal view of the skull of *Gymnallabes nops* (56.57mm SL) (MCZ 50298). ant: os antorbitale; apal: os autopalatinum; cl: os cleithrum; eoc: os exoccipitale; fr: os frontale; io-IV: os infraorbitale IV; leth: os latero-ethmoideum; meth: os mesethmoideum; mnd: mandibula; mx: os maxillare; ns: os nasale; op: os operculare; par-soc: os parieto-supraoccipitale; pp-v4: parapophysis of vertebra 4; prmx: os premaxillare; pt: os pteroticum; p-trc: transscapular process; pt-scl: os posttemporo-supracleithrum; pvm: os praevomerale; sph: os sphenoticum; spop: os suprapraeoperculare. *[Vue dorsale du crâne de* Gymnallabes nops. *ant : antorbital ; apal : autopalatin ; cl : cleithrum ; eoc : exoccipital ; fr : frontal ; io-IV : infraorbital IV ; leth : ethmoide latéral ; meth : mésethmoide ; mnd : mandibulaire ; mx : maxillaire ; ns : nasal ; op : operculaire ; par-soc : pariéto-supraoccipital ; pp-v4 : parapophyse de la quatrième vertèbre ; prmx : prémaxillaire ; pt : ptérotique ; p-trc : processus transscapulaire ; pt-scl : posttemporo-supracleithrum ; pvm : prévomer ; sph : sphénotique ; spop : suprapréoperculaire.]*

parasphenoid through one short interdigitating spine. It carries one tooth plate, which shows a constriction in the middle (Fig. 10).

Orbital region. - The circumorbital series is highly reduced, both in shape and the number of bones. Of the whole set of five bones present in most other clariids (Cabuy *et al*., 1999; Devaere *et al*., 2001), only the infraorbital IV and the antorbital are present in *Gymnallabes nops* (Figs 2, 3A) [for discussion on the nomenclature of the circumorbital bones in clariids, we refer to Adriaens *et al*. (1997)]. The antorbital bone is very small, lying dorso-posteriorly of the base of the maxillary barbel, close to the maxillary bone and dorsal to the rostral end of the autopalatine. The infraorbital IV is reduced to a more or less completely open, canal bone. This makes that the infraorbital canal runs almost completely unprotected along the lateral side of the head. This infraorbital bone has the most dorsal position of the neurocranial bones, elevated by the hypertrophied jaw adductor muscles.

The frontals (Figs 2, 3A) form the largest bones of the skull roof. The two contralateral parts are lying closely against each other, leaving a clear joint. The frontals enclose the anterior fontanel entirely, except for the anterior most border contacting the mesethmoid. The anterior fontanel separates the two frontals along the rostral half. Within this fontanel, the epiphyseal bridge is clearly visible; with the anterior part of the postpineal fontanel being exposed. The infraorbital canal exits the skull roof at the level of the frontals, close to the connection between the latter bone and the lateral ethmoid. The lateral side of the skull is formed by the

orbitosphenoid and pterosphenoid (Figs 3A, 3B, 4), which are ventrally connected to the parasphenoid (Fig. 3B). This latter bone runs from the rostral end of the orbital region up to the occipital region; it bears one elongated process.

Temporal region. - The skull roof in this region is formed by the frontals, the sphenotic and the pterotic (Fig. 2). The sphenotic (Figs 2, 3A) interdigitates rostro-medially with the frontal and caudally with the pterotic. The pterotic (Figs 2, 3A), in turn, contacts the parieto-supraoccipital on the medial side and the posttemporo-supracleithrum caudally. Both the sphenotic and pterotic lack lateral plates. They form a firm connection between the neurocranium and the suspensorium through a set of interdigitating processes. On the anterior side of the sphenotic one large and one small process are present. On the posterior side of the pterotic, two additional processes are present. In the pterotic, however, the largest process is situated most externally to the hyomandibula, which is opposite for the sphenotic spines. Ventrally, the neurocranium is formed by the paired prootics (Fig. 3B).

Occipital region. - The neurocranium is caudally bordered by the parieto-supraoccipital (Figs 2, 3A), bearing a medial, long, caudally pointed spine. This bony complex encloses the posterior fontanel, which is very small and lies in the caudal half of the parieto-supraoccipital. The posttemporo-supracleithrum (Figs 2, 3A) rostrally makes contact with the pterotic. Further, it is connected to the pectoral girdle and to the parapophysis of the fourth vertebra, through a solid transscapular process. Ventrally, this region of the skull consists of the exoccipitals and the basioccipitals (Fig. 3B).
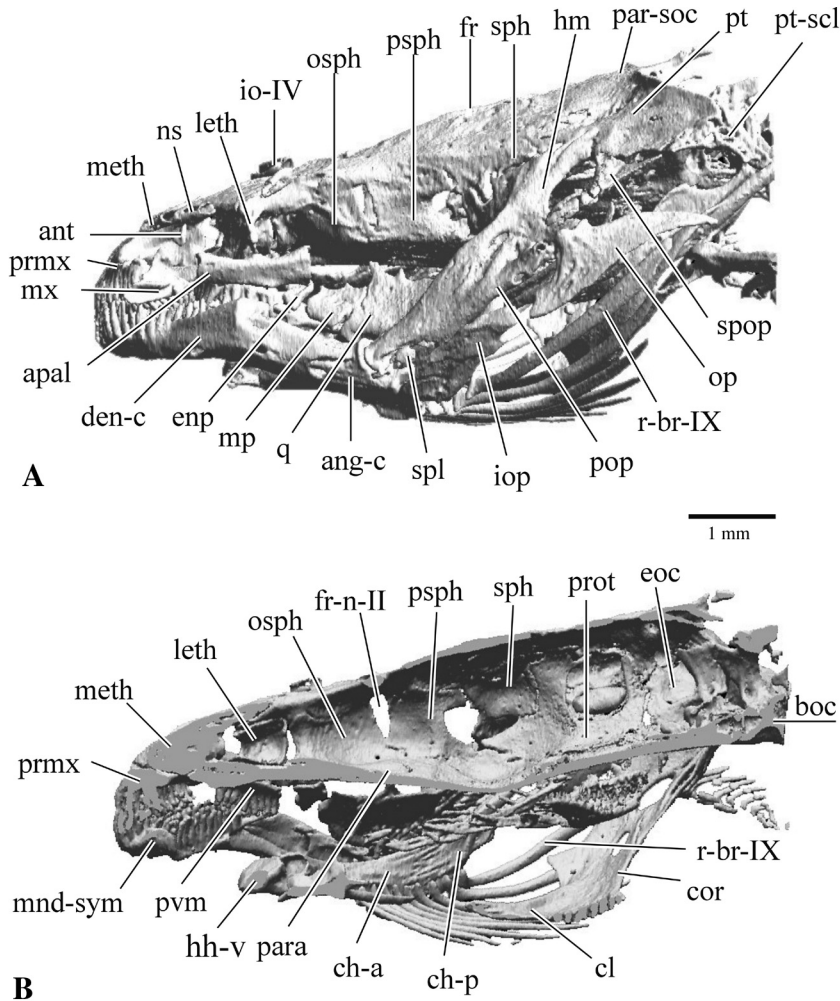
A

B

Figure 3. - Lateral view of the skull of *Gymnallabes nops* (56.57 mm SL) (MCZ 50298). **A**: Left lateral view; **B**: Sagittal view. ang-c: angular complex; ant: os antorbitale; apal: os autopalatinum; boc: os basioccipitale ; ch-a: os ceratohyale anterior; ch-p: os ceratohyale posterior; cl: os cleithrum; cor: os scapulo-coracoideum; den-c: dentary complex; enp: os entopterygoideum; eoc: os exoccipitale; fr: os frontale; fr-n-II: foramen of the optic nerve; hh-v: os hypohyale ventrale; hm: os hyomandibulare; iop: os interopercu-lare; io-IV: os infraorbitale IV; leth: os latero-ethmoideum; meth: os mesethmoideum; mnd-sym: mandibular symphysis; mp: os metapterygoideum; mx: os maxillare; ns: os nasale; op: os operculare; osph: os orbitosphenoideum; para: os parasphenoideum; par-soc: os parieto-supraoccipitale; pop: os praeoperculare; prmx: os praemaxillare; prot: os prooticum; psph: os pterosphenoideum; pt: os pteroticum; pt-scl: os posttemporo-supra-cleithrum; pvm: os praevomerale; q: os quadratum; r-br-IX: radius branchiostegus IX; sph: os sphenoticum; spl: os spleniale; spop: os suprapraeoperculare. *[Crâne de* Gymnal-labes nops. *A : Vue latérale ;* **B** *: Vue sagittale. ang-c : complexe angulaire ; ant : antor-bital ; apal : autopalatin ; boc : basioccipital ; ch-a : cératohyal antérieur ; ch-p : céra-tohyal postérieur ; cl : cleithrum ; cor : scapulo-coracoïde ; den-c : complexe dentaire ; enp : entoptérygoïde ; eoc : exoccipital ; fr : frontal ; fr-n-II : foramen du nerf optique ; hh-v : hypohyal ventral ; hm : hyomandibulaire ; iop : interoperculaire ; io-IV : infraor-bital IV ; leth : ethmoide latéral ; meth : mésethmoide ; mnd-sym : symphyse mandibu-laire ; mp : métaptérygoïde ; mx : maxillaire ; ns : nasal ; op : operculaire ; osph : orbit-osphénoïde ; para : parasphenoïde ; par-soc : pariéto-supraoccipital ; pop : pré-operculaire ; prmx : prémaxillaire ; prot : prootique ; psph : pterosphénoïde ; pt : ptéro-tique ; pt-scl : posttemporo-supracleithrum ; pvm : prévomer ; q : carré ; r-br-IX : rayon branchiostège IX ; sph : sphénotique ; spl : splénial ; spop : suprapréoperculaire.]*

Maxillary bones. - The premaxillaries (Figs 2, 3) are large, toothed plate-like bones. The anterior part of the pre-

maxillaries bears several rows of slightly curved teeth, while the posterior, some-what smaller, part remains teethless. The maxilla is a rod-like bone (Figs 2, 3A, 4). It has a little indentation, in which the base of the barbel is enclosed. The proxi-mal part of the maxilla is broader and bears two articulatory facets for the artic-ulation with the autopalatine.

Splanchnocranium

Lower jaw. - The lower jaw consists of two parts: the dentary and the angular complexes (Figs 3A, 4). The coronoid process on the lower jaw is distinct and firm. The anterior part of the lower jaw is covered with a large tooth battery, with slightly curved teeth, which run close up to the top of the coronoid process. The lower jaw shows five pores for branches of the preopercular-mandibular canal. The well-developed retroarticular process lies mostly ventral from the articulation facet of the quadrate. The lower jaw embeds the rostral end of the preoperculo-mandibular canal of the lateral line system. The first three pores (PM1-3) lie in the dento-splenio-mentomeckelium complex, the fourth (PM4) is situated on the border of both bone complexes, while the fifth one (PM5) is located on the caudal end of the lower jaw.

Suspensorium. - The suspensorium consists of the hyomandibula, quadrate, entopterygoid, metapterygoid and the pre-opercle (Figs 3A, 5A). This latter bone is mentioned here since it is fused to the sus-pensorium and forms one functional unit. The hyomandibula connects to the sphe-notic and the pterotic through a set of pro-cesses. At the level of the sphenotic, a plate-like process is present anteriorly, followed by a smaller, pointed process. On the caudal side of the articulation ridge, three processes are present, rostral-ly to caudally, in size increasing for the interdigitation with the pterotic. Between these two sets of processes an articulation ridge is present, making contact only with the sphenotic bone. On the lateral side, a clear ridge is present, inclosing a foramen. On the rostral side of the hyomandibula no plate-like outgrowth is present.
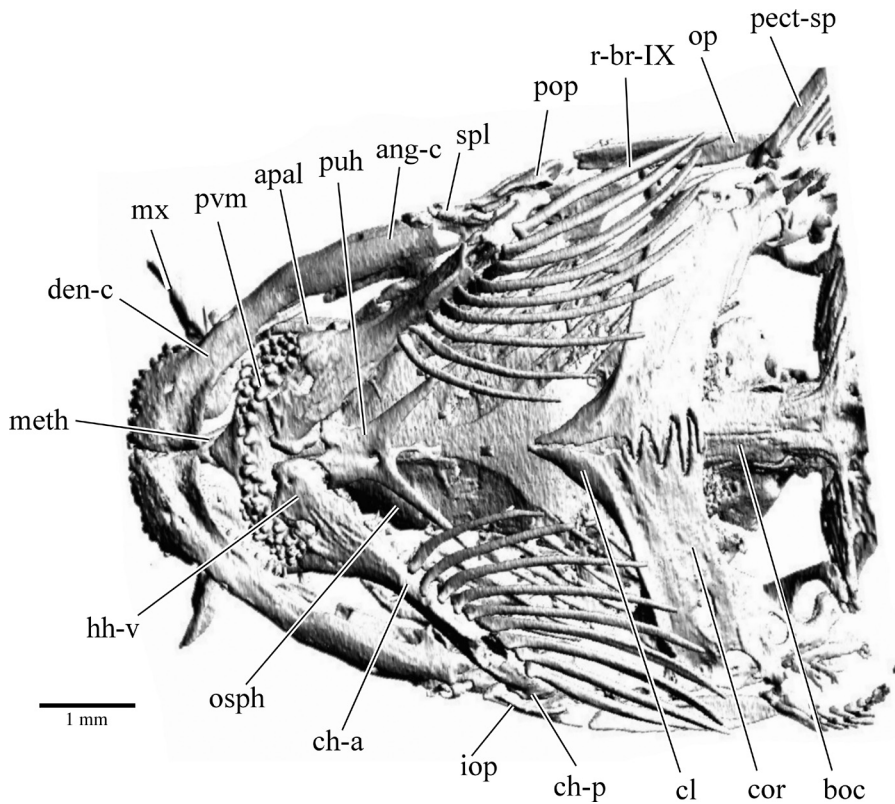
Figure 4. - Ventral view of the skull of *Gymnallabes nops* (56.57 mm SL) (MCZ 50298). ang-c: angulare complex; apal: os autopalatinum; boc: basioccipitale; ch-a: os ceratohyale anterior; ch-p: os ceratohyale posterior; cl: os cleithrum; cor: os scapulo-coracoideum; den-c: dentary complex; iop: os interoperculare; hh-v: os hypohyale ventrale; meth: os mesethmoideum; mx: os maxillare; op: os operculare; osph: os orbitosphenoideum; pect-sp: pectoral spine; pop: os praeoperculare; pvm: os praevomerale; puh: os parurohyale; r-br-IX: radius branchiostegus IX; spl: os spleniale. *[Vue ventrale du crâne de* Gymnallabes nops. *ang-c : complexe angulaire ; apal : autopalatin ; boc : basioccipital ; ch-a : cératohyal antérieur ; ch-p : cératohyal postérieur ; cl : cleithrum ; cor : scapulo-coracoïde ; den-c : complexe dentaire ; iop : interoperculaire ; hh-v : hypohyal ventral ; meth : méséthmoide ; mx : maxillaire ; op : operculaire ; osph : orbitosphénoïde ; pect-sp : épine pectorale ; pop : préoperculaire ; pvm : prévomer ; puh : parurohyal ; r-br-IX : rayon branchiostège IX ; spl : splénial.]*

The opercular process is ventro-caudally oriented. The quadrate ventro-laterally contacts with the lower jaw through a well-developed articulation head. It makes a clear contact with the complete caudal side of the metapterygoid bone; dorsally this occurs through an interdigitation zone, ventrally through a synchondrosis. On the other hand no contact between the quadrate and the entopterygoid can be observed, as they are completely separated by the metapterygoid. The last bone is the preopercle (see below), which is completely incorporated in the suspensorium. This bone surrounds a part of the preoperculo-mandibular canal, and shows two pores (PM5-6).

The autopalatine bone (Figs 2, 3A, 4) shows a clear concave medial side, with a rostral and caudal cartilaginous tip. The autopalatine lies ventrolateral to the lateral ethmoid and shows a clear and well-pronounced articulation facet at the articulation site with the lateral ethmoid. On the rostral side it articulates with the maxillary bone, thus being part of the palatine-maxillary mechanism. A single, small, tubular, splenial bone (Adriaens *et al.*, 1997) lies laterally to the articulation between the lower jaw and the quadrate (Figs 3A, 4).

Hyoid arches. - The hyoid arch consists of two anterior and posterior ceratohyals and two ventral hypohyals (Figs 3B, 4). On the scans there was no evidence of the dorsal hypohyals, this could be due to decalcification, since in other clariids the dorsal hypohyals are present (Cabuy *et al.*, 1999; Devaere *et al.*, 2001, 2004). Ventrally, the hyoid arch articu-

lates with nine branchiostegal rays. The first six branchiostegal rays articulate with the ventral rim of the anterior ceratohyal, the following ray is placed at the small cartilaginous region between the anterior and posterior ceratohyals. The last two rays are situated on the posterior ceratohyal. The parurohyal lies in between the two hyoid arches and bears two caudo-lateral processes and one very small, spiny, caudal process (Fig. 4).

Branchial arches. - The "Bauplan" of the branchial basket corresponds to the general clariid situation. Only the size and the number form somewhat an exception to this general situation. The gill rakers in *Gymnallabes nops* are not only small, but also occur in small numbers. For a detailed description of this general configuration in clariids, we refer to Adriaens and Verraes (1998).

Opercular series. - The opercular bone is a triangular, caudally, pointed structure (Fig. 3A). On the rostro-dorsal side it bears a large articulatory facet for the articulation with the hyomandibula. Caudally to this facet, a large process is present. On the medial side of the caudal part, a ridge is present, presumably for the attachment of the levator operculi muscle. On the rostro-ventral side of the articulation facet, a large, more plate-like, extension is present, ending on a border at the contact zone with the interopercular bone. This latter bone is situated between the opercular bone and the lower jaw (Fig. 3A). On the medial side, the interopercle bears a marked concavity enclosing the caudal tip of the posterior
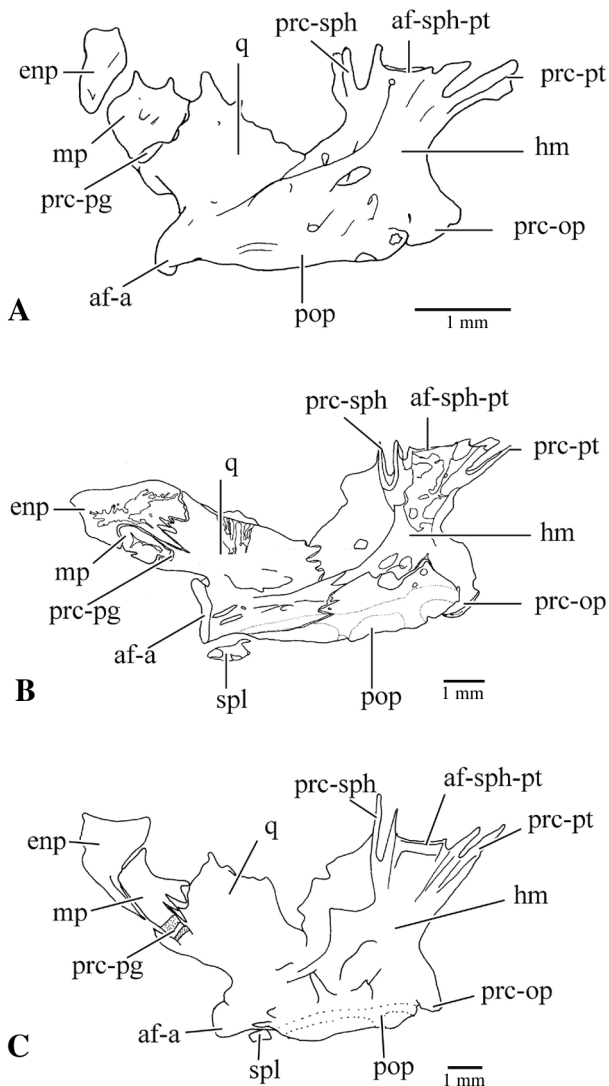
Figure 5. - Lateral view of the suspensorium. **A**: *Gymnallabes nops* (56.57 mm SL) (MCZ 50298); **B**: *Channallabes apus* (28 mm SL) (MRAC 175247-270); **C**: *Gymnallabes typus* (192 mm SL) (MRAC 97-030-P-0010). af-a: articulatory facet of the quadrate with the angulo-splenio-articulo-retroarticular; af-sph-pt: articulatory facet of the hyomandibula with the sphenotic and the pterotic; enp: os entopterygoideum; hm: os hyomandibulare; mp: os metapterygoideum; pop: os praeoperculare; prc-op: opercle process; prc-pg: pterygoid process; prc-pt: pterotic process; prc-sph: sphenotic process; q: os quadratum; spl: os spleniale. *[Vue latérale du suspensorium de **A** :* Gymnallabes nops*; **B** :* Channallabes apus*; **C** :* Gymnallabes typus*. af-a : face articulaire du carré avec l'angulo-splénial-articulo-rétroarticulaire ; enp : entoptérygoïde ; hm : hyomandibulaire ; mp : métaptérygoïde ; pop : préoperculaire ; prc-op : processus operculaire ; prc-pg : processus ptérygoïdien ; prc-pt : processus ptérotique ; prc-sph : processus sphénotique ; q : carré ; spl : splénial.]*

ceratohyal. Laterally, on top of the jaw muscles, two suprareopercular (Figs 2, 3A) bones are present. The larger, dorsally situated suprapreopercular bone shows a triangular shape. The ventral one is reduced to a tubular bone, enclos-

ing the preopercular canal. As mentioned above, the praeopercular bone is incorporated in the suspensorium (Fig. 3A).

Postcranial skeleton

Vertebrae. - The total number of vertebrae is 62 (Fig. 6) (including those comprised by the Weberian apparatus). There are 18 precaudal vertebrae, of which five carry ribs. The dorsal fin comprises a total of 75 fin rays; 59 fin rays are present in the anal fin. A little foramen can be found at the bases of the parapophyses of the first precaudal vertebrae.

Pectoral girdle. - The pectoral girdle comprises a scapulo-coracoid and a cleithral bone (Figs 3B, 4), which are strongly sutured to each other. Ventrally, the two contralateral parts are strongly connected to each other. In the caudal part, this occurs through several large processes. A clear fenestra is present between the right cleithral and scapulo-coracoid bone, but completely absent in the left part (Fig. 4). The cleithral bone shows a clear anterior process, as well as a ridge on its rostro-ventral side. On the scapulo-coracoid, a distinct insertion ridge is present for the attachment of the pectoral muscles. The pectoral fin has a non-serrated spine and eight fin rays that articulate with the two radials present.

Pelvic girdle. - Although the pelvic girdle is highly decalcified, the basipterygium shows two clear processes (internal and external anterior process: see Arratia 2003). No more than four pelvic fin rays can be discerned.

Caudal skeleton. - The caudal skeleton (Fig. 7) consists out of the parhypural, five hypurals, urostyl and uroneural, which are all fused in a single bony plate. Dorsally to this fusion lies the broad tipped, epural. The neural spine of the second preural vertebra is elongated, broadly tipped and supports the caudal fin rays; the neural spine of the third preural vertebra is also elongated but ends with a spiny tip and does not support the dorsal fin rays. This supporting function is performed by a pterygiophore. Both haemal spines of the second and third preural vertebrae are elongated, broad and support the anal fin rays. Anteriorly, the dorsal and anal fin rays are supported by pterygiophores.

<center>

DISCUSSION

</center>

Original description

In the original description of Roberts and Stewart (1976), containing some metric and meristic data, the holotype of *Gymnallabes nops* was included in the genus *Gymnallabes* Günther, 1867. At that time this genus included *Gymnallabes typus* Günther, 1867; *G. alvarezi* Roman, 1970 and *G. tihoni* (Poll, 1944) of which the latter was later transferred to *Platyallabes* Poll, 1977. Although the largest similarity was observed between *G. nops* and *Platyallabes tihoni*, the
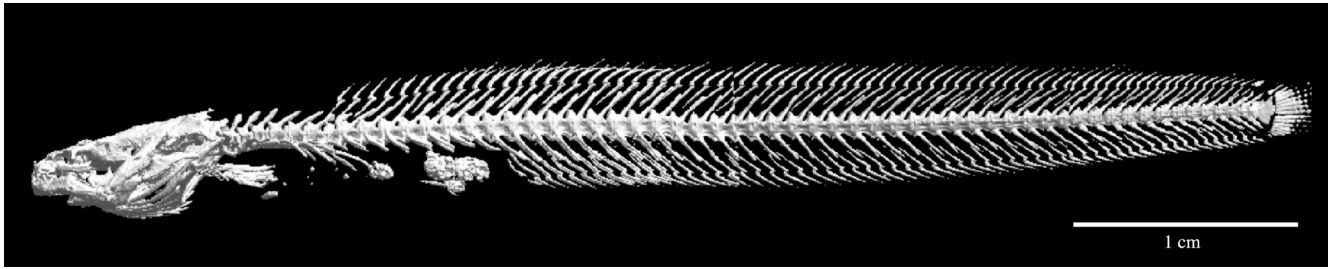
Figure 6. - Overall lateral view of *Gymnallabes nops* (56.57 mm SL) (MCZ 50298). *[Vue latérale générale de* Gymnallabes nops.*]*
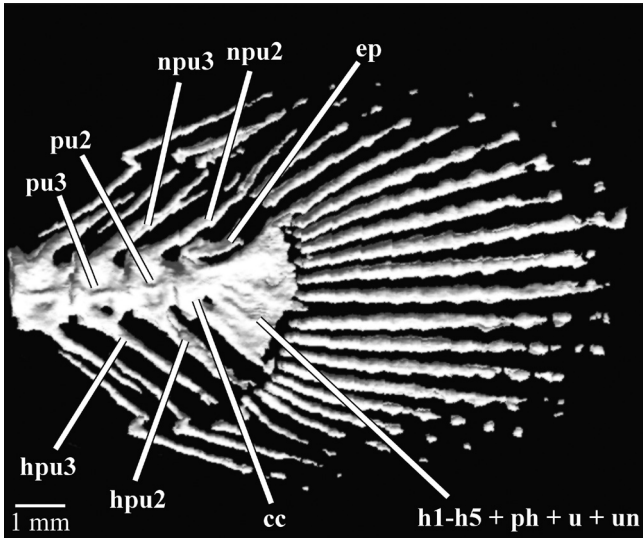

Figure 7. - Caudal skeleton of *Gymnallabes nops* (56.57 mm SL) (MCZ 50298). cc: composed centre; ep: os epurale; h1-h5 + ph + u + un: complex of os hypural 1 to 5, parhypural, urostyl and uroneural; hpu2, 3: haemal spine of preural vertebrae 2, 3; npu2, 3: neural spine of preural vertebrae 2, 3; pu2, 3: preural centre 2, 3. *[Squelette caudal de* Gymnallabes nops. *cc : centre composé ; ep : épural ; h1-h5+ph+u+un : complexe terminal (hypuraux 1 à 5 + parhypural + urostyle + uroneural) ; hpu2, 3 : épine hémale des vertèbres préurales 2, 3 ; npu2, 3 : épine neurale des vertèbres préurales 2, 3 ; pu2, 3 : centres préuraux 2, 3.]*

authors pointed out that a comprehensive set of differences existed. Most of them, however, proved to be invalid, as this study indicates, simply by taking more specimens of *P. tihoni* into account (see below).

The authors gave as a first striking difference the lack of eyes in *G. nops*. This is not unique and also occurs in *Platyallabes tihoni* (MCZ 88947, 50297). A second character used was the observation that the pectoral and pelvic fins did not extend respectively beyond the origin of the dorsal and anal fin, in contrast to the situation in *P. tihoni*. In our data set (Tab. I) a large variation on the length of both pectoral and pelvic fins in *P. tihoni* was observed, a variation already shown in several other anguilliform clariids (Adriaens *et al.*, 2002). Paired fins not reaching or reaching further than the origin of the respectively dorsal and anal fin could both be found. Also the length of the innermost pelvic fin ray in *P.*

tihoni shows a lot of variation and is not always extremely reduced, as stated in the original description. Further, it was stated that *G. nops* has a higher abdominal body depth and caudal peduncle depth, shorter pectoral spine and a smaller skull roof width, but all these lie within the ranges of *P. tihoni* (Tab. I). The distance between the occipital process and the dorsal fin was given as a last metric difference. This was stated to be double in *G. nops* compared to *P. tihoni*. Since a small distance is one of the distinctive characters of *P. tihoni* (Devaere, personal observation), the distance is larger in *G. nops* but not twice that of *P. tihoni* (Tab. I).

Since metric and meristic data of *Gymnallabes nops* overlap, mostly lying within the range of *Platyallabes tihoni*, the question raises if *G. nops* is still a valid species. Furthermore, since *Platyallabes* has become a different, monotypic genus, the question raises if *G. nops* is designated to the proper genus. A discussion on shared characters follows, based on the obtained morphological characters.

Diagnosis

Principal Components Analysis

For the analysis, we examined 110 specimens of the wide area around the type locality of *G. nops*. This region includes the lower Congo stream up to Kinshasa, Southern West Coastal Equatorial, and the Kasai region (Thieme *et al.*, 2005). These include specimens of *Channallabes apus* (n = 29), *Platyallabes tihoni* (n = 39), *Platyclarias machadoi* (n = 21), *Gymnallabes alvarezi* (n = 1) with type material of *Gymnallabes nops*, *Platyallabes tihoni* and *Platyclarias machadoi*. We also included the specimens of *Gymnallabes typus* (n = 19), from the Niger delta, Northern and Central West Coastal Equatorial Freshwater Ecoregion (Thieme *et al.*, 2005) (includes *G. typus* types).

Figure 8 plots the second principle component derived from a PCA on the covariance matrix for 25 measurements against the first principle component derived from a correlation matrix of 5 meristic characters. The dominant characters for the second principal component are the distance between the occipital process and the dorsal fin, the caudal peduncle depth and the barbel lengths; while for the first component, the total number of vertebrae and the number of ribs are the

Table I. - Measurements and meristic data for the holotype of *Gymnallabes nops*, compared to *Platyallabes tihoni, Gymnallabes typus* and *Gymnallabes alvarezi*. Abbreviations used are explained in the text. *[Mesures et données méristiques de l'holotype de* Gymnallabes nops, *comparées à celles de* Platyallabes tihoni, Gymnallabes typus *et* Gymnallabes alvarezi. *Les abréviations sont expliquées dans le texte].*

	G. nops	P. tihoni					G. typus					G. alvarezi				
		n	min	max	mean	SD	n	min	max	mean	SD	n	min	max	mean	SD
TL (mm)	61.0	54	63	380			32	49	284			18	35.5	329		
SL (mm)	56.6	54	58	359			32	44	259			18	31	318		
Measurements in % standard length																
PaL	40.3	54	18.6	34.7	26.3	3.5	32	29.2	37.1	32.9	2.2	18	24.1	40.6	34.9	4.2
PPcL	16.4	54	8.3	17.0	12.1	2.0	32	10.0	19.3	13.0	1.9	18	8.2	20.8	15.6	3.3
PPvL	35.0	54	18.3	30.6	23.5	3.1	32	27.2	36.2	30.5	2.3	18	32.0	37.8	34.7	2.3
PdL	24.8	54	12.5	23.4	16.9	2.8	32	18.1	27.8	21.6	2.4	18	16.9	35.9	28.3	4.6
SPDFL	8.7	54	2.2	6.6	3.7	1.0	32	5.2	11.2	8.3	1.5	18	8.3	15.8	11.9	1.7
PcFL	9.4	54	4.6	9.9	6.6	1.3	32	3.8	8.5	5.7	1.0	18	3.6	11.3	8.0	2.4
PcSL	5.1	54	3.3	7.0	5.0	0.8	32	1.8	3.8	2.5	0.5	18	1.6	4.6	3.5	0.9
PvFL	5.6	54	4.0	7.3	5.6	0.8	32	1.7	6.8	4.2	0.9	18	3.8	7.0	5.5	1.0
CPD	3.4	54	1.1	3.6	1.9	0.5	32	1.9	4.5	3.0	0.7	18	1.9	5.9	4.0	1.0
ABD	6.6	54	3.0	6.4	4.2	0.8	32	4.6	7.8	6.3	0.8	18	4.8	11.6	8.4	1.9
IpcD	11.7	54	6.9	13.0	9.3	1.5	32	5.9	11.0	8.0	1.1	18	2.2	4.9	3.3	0.8
IpvD	4.8	54	2.9	6.2	4.2	0.8	32	1.4	4.0	2.5	0.6	18	5.8	15.7	11.3	3.1
SkL	15.1	54	7.4	17.2	12.7	2.1	32	11.1	18.0	13.1	1.6	18	7.5	27.0	18.3	5.6
Measurements in % head length																
PoL	*	54	61.2	85.5	74.7	9.2	32	62.0	74.0	67.7	2.4	18	62.5	86.9	74.5	6.7
SpL	13.6	54	6.9	20.3	13.5	3.0	32	10.2	20.0	15.5	2.6	18	13.0	28.6	20.1	3.1
SkW	68.7	54	62.9	113.9	75.8	7.9	32	52.1	69.6	60.3	4.6	18	45.4	88.5	59.5	10.6
SpW	26.0	54	10.2	22.3	16.0	3.0	32	12.1	27.3	18.8	4.0	18	18.6	33.6	26.8	4.1
IoD	*	54	30.4	56.9	38.5	4.5	32	24.6	40.4	33.0	3.5	18	24.9	41.9	30.8	4.0
ANID	19.4	54	10.5	26.1	14.1	2.7	32	10.6	19.0	15.0	2.2	18	12.1	20.7	16.4	2.0
PNID	33.3	54	22.6	44.8	31.2	4.5	32	23.1	34.1	27.7	2.8	18	23.3	39.6	28.6	3.9
RSkW	45.3	54	30.3	69.0	40.0	7.4	32	28.9	53.4	42.0	5.5	18	25.6	46.0	35.4	5.3
OSkW	58.6	54	43.7	92.9	54.9	6.8	32	42.5	60.8	51.4	3.4	18	40.0	59.7	47.5	4.6
SkH	45.5	54	22.8	61.7	34.6	6.9	32	26.6	49.8	40.0	5.8	18	33.1	129.7	46.7	21.5
ED	*	54	3.7	12.8	6.1	1.6	32	4.1	8.4	6.5	1.1	18	6.7	11.8	8.8	1.4
SnH	20.3	54	9.5	21.6	13.3	4.8	32	10.0	18.5	14.2	2.0	18	7.7	25.9	14.1	3.9
OSkH	23.4	54	16.8	44.0	23.4	4.8	32	17.5	36.0	26.0	4.6	18	17.1	35.6	25.1	5.0
PhL	27.7	54	17.2	44.5	27.6	4.1	32	18.6	31.8	24.5	3.5	18	19.1	48.1	26.2	6.3
IMnID	22.4	54	20.3	42.0	27.5	3.7	32	18.5	37.1	24.4	3.5	18	13.2	33.1	21.4	4.4
EMnID	45.5	54	32.1	67.8	43.2	6.0	32	31.5	44.6	39.3	3.6	18	24.9	44.1	34.0	5.2
MW	26.1	54	19.5	76.1	32.7	8.5	32	21.5	39.3	30.8	4.0	18	19.0	36.4	27.9	5.3
SkR	11.3	54	9.5	26.8	18.9	4.6	32	4.0	44.1	15.7	9.5	18	11.5	57.8	25.7	11.4
Meristic counts																
RB	5	33	4	7	5	0.6	22	6	12	8.6	1.7	3	10	14	12	2
TV	62	33	63	83	74	5.7	22	78	92	84	2.7	3	71	99	81	11

two most important. This reveals the presence of several groups that do not overlap. In this plot *Gymnallabes nops* takes a separate position, apart from other groups and type material, indicating that *G. nops* is indeed a valid species.

Diagnosis

    Gymnallabes nops differs from all other anguilliform clariids by the combination of following characters: a large rostral outgrowth of the hypertrophied adductor mandibulae complex; a reduced infraorbital series, both in number and size; the absence of the medial expansions of the frontal plates, leaving the epiphyseal bridge clearly exposed; the entopterygoid situated in a completely rostral position of the metapterygoid, a short posterior process on the prevomer
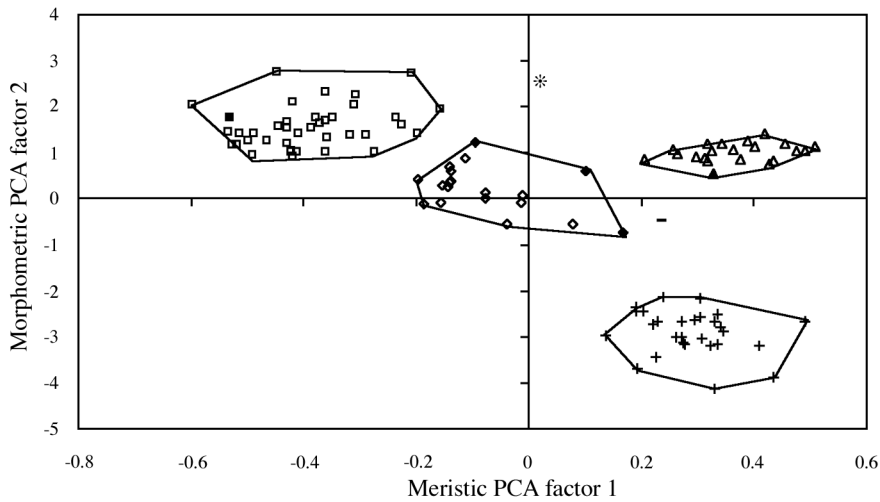
Figure 8. - Combined plot of the second principal component derived from a PCA of 25 log-transformed metric variables against the first principal components of a PCA using 5 meristic variables. ⚹ *Gymnallabes nops*; + *Channallabes apus*; ● *Gymnallabes alvarezi*; ◆ syntypes of *Gymnallabes typus*; ◇ other specimens of *Gymnallabes typus*; ▲ holotype of *Platyclarias machadoi*; △ paratypes of *Platyclarias machadoi*; ■ holotype of *Platyallabes tihoni*; □ other specimens of *Platyallabes tihoni*. [*Graphique d'une analyse en composantes principales, basée sur 25 variables métriques (log-transformé) (PC2) et 5 variables méristiques (PC1).* ⚹ Gymnallabes nops *; +* Channallabes apus *; ●* Gymnallabes alvarezi *; ◆ syntypes de* Gymnallabes typus *; ◇ autres spécimens de* Gymnallabes typus *; ▲ holotype de* Platyclarias machadoi *; △ paratypes de* Platyclarias machadoi *; ■ holotype de* Platyallabes tihoni *; □ autres spécimens de* Platyallabes tihoni.*]*
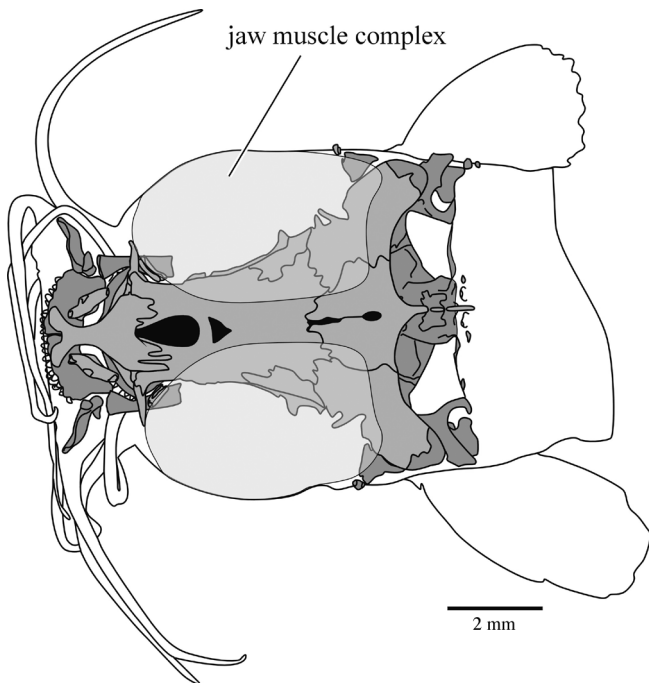

Figure 9. - Dorsal view of the skull of *Gymnallabes nops* (56.57 mm SL) (MCZ 50298), with indication of the position of the adductor mandibulae complex (shaded) and the degree it covers the skull roof. *[Vue dorsale du crâne de* Gymnallabes nops, *avec indication de la position du complexe adducteur mandibulaire (hachuré) et du degré de couverture du toit crânien].*

and a large rostro-ventral process on the opercle.

Although the absence of the eyes is not unique, it has some typical consequences; the available orbital space is taken by an outgrowth of the hypertrophied adductor mandibulae complex, covering the lateral and dorsal side of the skull (Fig. 9). Since no discrimination between soft tissues is possible on radiographies or CT-scan, we have no certainty that nothing of the visual sense organ is developed. It cannot be overruled that the eyes could have developed up to a certain embryonic stage, but remain invisible as they are covered by the integument. A comparable situation has been observed in *Caecomastacembelus brichardi* (Poll, 1973). The only certainty that we have obtained through the CT-scans is that the foramen for the optic nerve is clearly present between the orbitosphenoid and the pterosphenoid (Fig. 3B), which could indicate the passage of an optic nerve and thus a certain level of development of the visual sense organ itself.

As in other anguilliform species, as well as in *Uegitglanis* and the primitive catfish family Diplomystidae (David, 1936; Arratia, 1987), the plesiomorphic state of a reduced series of circumorbital bones occurs in *G. nops*. However, this reduction in *G. nops* not only involves a reduction of the plate-like expansions on each of the infraorbital bones, but is also reflected in a reduction of the number of infraorbital bones. Only the first and last one are still present, namely the antorbital and infraorbital IV (Figs 2, 3A). Those two are the most dorsally situated bones and are also the only circumorbital bones present in *Dolichallabes microphthalmus* (Devaere *et al.*, 2004). As was stated in Devaere *et al.* (2004) this could be due to a heterochronic process, although for *G. nops* some other reasons for this reduction could be suggested. Since *G. nops* shows no evidence of eyes, a protecting series of bones around the orbital region is not required. This, however, leaves the infraorbital canal unprotected. Although, a discontinuous infraorbital canal does sometimes occur (Webb, 1989), this seems not to be the case here. There is no evidence of a discontinuous canal in clariids (Adriaens *et al.*, 1997; Cabuy *et al.*, 1999; Devaere *et al.*, 2001) Furthermore, the absence of the infraorbital bones II and III could also be linked to the subsequent outgrowth of the jaw muscle complex (Fig. 9). Another explanation is that the

reduced number of infraorbital bones in the reconstruction is an artifact due to decalcification of those small bones, which makes them indistinguishable for CT-scanning. But as other small bones are still present (cf. nasal and splenial bones) this seems very unlikely.

Furthermore, in *G. nops* the plates on the frontals, medially overgrowing the anterior fontanel are absent, leaving the epiphyseal bridge clearly visible (the cartilaginous bridge, however, is still enclosed by a bony case formed by the frontals) (Adriaens and Verraes, 1998). The typical posterior process on the prevomer is rather short, in contrast to the long process present in *Gymnallabes typus* and *Channallabes apus* (Devaere *et al*., 2001) (Fig. 10A-C). Also, on the prevomer a single tooth plate is present, as is frequently the case in other adult clariids. In *Gymnallabes nops*, however, the tooth plate shows a constriction in the middle, almost dividing the tooth plates in two (Fig. 10A). Additionally, the configuration of the entopterygoid and the metapterygoid is typical in *G. nops*. The entopterygoid lies in a completely rostral position of the metapterygoid, with no dorsal or ventral contact zone (Fig. 5). The entopterygoid and metapterygoid lie somewhat separate from each other but remain attached through a sheet of connective tissue (Fig. 5). A last unique trait is the large rostro-ventral process on the opercle (Fig. 3A). In other anguilliform clariids the extension anterior of the articulation facet of the opercle with the hyomandibula is shorter.

Description of *Gymnallabes nops*

The proportional measurements and counts are given in table I. *Gymnallabes nops* is characterized by an elongated, in cross-section round, body with a dorso-ventrally flattened head. The degree of anguilliformity can be expressed as the ratio of the total length to the body height (Poll, 1942). This ratio, in the holotype of *G. nops*, is 15.2 with a postanal length of 59.7% of the standard length.

The most striking character is that *Gymnallabes nops* show no external evidence of the presence of eyes (Fig. 1). The orbital region is occupied by an anterior outgrowth of the hypertrophied adductor mandibulae complex. The dorsal outgrowth of this muscle complex makes that the skull roof is largely covered (Fig. 9). The in alcohol preserved holotype of *G. nops* shows an evenly light brownish/pinkish coloration, but not a total depigmentation as was stated in the original description. Both paired and impaired fins and the nostrils show an even lighter brown color. Only near the barbels, no pigmentation can be observed and the cartilage present in the barbels is visible through the skin (Fig. 1).

The skull length is 15.1% of the standard length. The skull width is 68.7% of the skull length. Two large jaw muscles, slightly bulging out, further characterize the head. This makes that only a small part of the skull roof is visible
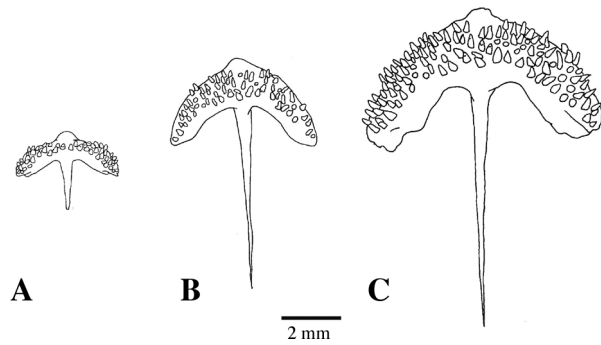

Figure 10. - Ventral view of the prevomer. **A**: *Gymnallabes nops* (56.57 mm SL) (MCZ 50298); **B**: *Channallabes apus* (258mm SL) (MRAC 175247-270); **C**: *Gymnallabes typus* (199mm SL) (MRAC 92-083-P-0035-0036). [*Vue ventrale du prévomer*.]

(11.3% of the skull length).

In the skull roof, both anterior and posterior fontanel are present. The anterior fontanel can be located by the presence of double set of pores of the supraorbital canal (S4). Behind these two pores, also the next pair of pores (S5) of the supraorbital canal are clearly visible.

The unpaired fins form one continuous finfold. The dorsal fin originates at a considerable distance of the supraoccipital process (SPDFL is 8.7% of SL). The paired fins are both well developed. The pectoral fins have a length of 9.4% of the standard length. Also the pectoral spine is clearly visible and is 53.8% of the total pectoral fin length. The pelvic fins are 5.6% of the standard length.

The rostrally situated lips are fused in the mouth corners, upper and lower lips are of equal length.

Comparison with other clariids

For the comparison with other anguilliform representatives, we used the two species, to which *Gymnallabes nops* shows the greatest affinity: *Platyallabes tihoni* and *Gymnallabes typus*, as well as two other elongated species: *Channallabes apus* and *Dolichallabes microphthalmus*. In this paper we use *G. typus* as the only representative of the genus *Gymnallabes* to compare with *G. nops*. This due to the questionable generic placement of *Gymnallabes alvarezi* (Roman, 1970) (research on the systematic position of *G. alvarezi* is in progress). *G. nops* is characterized by a reduced skull, the presence of hypertrophied jaw muscles and the narrow part of the skull roof, in between the jaw muscles (Fig. 9). This corresponds to the general cranial morphology of anguilliform species (Cabuy *et al*., 1999; Devaere *et al*., 2001). For the comparison of the general morphology of *G. typus*, *C. apus* and *D. microphthalmus* we refer respectively to Cabuy *et al*. (1999), Devaere *et al*. (2001, 2004) and *P. tihoni* (Devaere, pers. obs.).

Besides a whole set of symplesiomorphic characters with the other anguilliform species, *G. nops* shows several char-

acters states that differ only with *P. tihoni*. Such characters involve the clearly constriction of the mesethmoid bone, caudally from the two rostral wings (comparable to most anguilliform species, except for *Platyallabes tihoni* were the constriction is less pronounced). *G. nops* has the general anguilliform lower jaw morphology with a tooth battery running up to a distinct coronoid process (Fig. 3A) (Devaere *et al.*, 2001, 2004). Only *Platyallabes tihoni* shows a less developed coronoid process. Further at the level of the suspensorium the interdigitation with the neurocranium occurs through two sets of processes, two anterior and three posterior processes, increasing in size from rostral to caudal. This configuration also viewed in *Gymnallabes typus* and in some specimens of *Channallabes apus*.

Next to the above mentioned differences, *G. nops* shows a set of similarities only with *P. tihoni*. The premaxilla, which is supported by the mesethmoid, has a small, posterior, plate-like extension, as only viewed in *P. tihoni*. Two processes are present on the sphenotic and pterotic for the interdigitation with the suspensorium (Fig. 3A). On the caudal side of the parieto-supraoccipital bone, which embeds a very small posterior fontanel, a somewhat short, pointed process is present. Further, no bony plate is present on the rostral side of the hyomandibula. A last similarity is that the opercular process is ventro-caudally orientated, comparable to the position in *P. tihoni*. The number of pre-caudal and total number of vertebrae of *G. nops* lies within the range of that in *P. tihoni*. The total number of vertebrae in *Gymnallabes typus* is higher than that in *G. nops* (Tab. I). Since the number of specimens on which gill rakers, dorsal and anal fin rays have been counted is small, no conclusive results can be given.

Geographic distribution

The type locality of *Gymnallabes nops* is near Tadi, about 50 km downstream from Luozi, along the lower stream of the Congo River, Democratic Republic of Congo (lat 5°14'S, long 13°56'). This is situated in the Lower Congo Rapids freshwater Ecoregion (Thieme *et al.*, 2005). *Platyallabes tihoni* occurs mostly in the same freshwater ecoregion, but also in the vicinity of Stanley Pool (Kinshsa region) and more downstream on the lower Congo. In contrast, *Gymnallabes typus* occurs nowhere near those localities or the Congo River. Most *G. typus* can be found near the Niger delta and in Cameroon. Even when incorporating the localities of the questionable *Gymnallabes alvarezi*, there is still no presence of other species of the *Gymnallabes* genus in the Congo basin. The similar biogeographical distribution of *G. nops* with *P. tihoni* and clear allopatry with other *Gymnallabes* species can be an additional indication of the wrong systematic position of *G. nops*, besides several synapomorphies with *P. tihoni* (ongoing study).

The above mentioned results show that *Gymnallabes*

nops can indeed be considered a valid species based on both metric and meristic measurements. This is additionally shown through a set of synapomorphies based on the osteology revealed by CT scanning. These morphological results, however, fail to unambiguously determine the correct taxonomic position. Further research on other clariids (including the other *Gymnallabes* species) will hopefully bring more clarity.

REFERENCES

ADRIAENS D. & W. VERRAES, 1998. - Ontogeny of the osteocranium in the African catfish, *Clarias gariepinus* (1822) (Siluriformes: Clariidae): Ossification sequence as a response to functional demands. *J. Morphol.*, 235: 183-237.

ADRIAENS D., VERRAES W. & L. TAVERNE, 1997. - The cranial lateral-line system in *Clarias gariepinus* (Burchell, 1822) (Siluroidei: Clariidae): Morphology and development of canal related bones. *Eur. J. Morphol.*, 35: 181-208.

ADRIAENS D., AERTS P. & W. VERRAES, 2001. - Ontogenetic shift in mouth opening mechanisms in a catfish (Clariidae, Siluriformes): A response to increasing functional demands. *J. Morphol.*, 247: 197-216.

ADRIAENS D., DEVAERE S., TEUGELS G.G., DE KEGEL B. & W. VERRAES, 2002. - Intraspecific variation in limblessness in vertebrates: A unique example of microevolution. *Biol. J. Linn. Soc.*, 75: 367-377.

ARRATIA G., 1987. - Description of the primitive family Diplomystidae (Siluriformes, Teleostei, Pisces): Morphology, taxonomy and phylogenetic implications. *Bonn. Zool. Monograph.*, 24: 1-120.

ARRATIA G., 2003. - The siluriform postcranial skeleton. An overview. *In*: Catfishes (Arratia G., Kapoor A.S., Chardon M. & R. Diogo, eds), pp. 121-157. Enfield, NH and Plymouth, UK: Science Publishers, Inc.

BOOKSTEIN F.L., CHERNOFF B., ELDER R., HUMPHRIES J., SMITH G. & R. STRAUSS, 1985. - Morphometrics in evolutionary biology. The geometry of size and shape change, with examples from fishes. *Philad. Acad. Nat. Sci.*, Spec. Publ., 1-277.

BOULENGER G.A., 1911. - Catalogue of the Fresh-water Fishes of Africa in the British Museum (Natural History). 2, 529 p. London: Printed by order of the Trustees.

CABUY E., ADRIAENS D., VERRAES W. & G.G. TEUGELS, 1999. - Comparative study on the cranial morphology of *Gymnallabes typus* (Siluriformes: Clariidae) and their less anguilliform relatives, *Clariallabes melas* and *Clarias gariepinus*. *J. Morphol.*, 240: 169-194.

DAVID L., 1936. - *Uegitglanis*, silure aveugle de la Somalie italienne : chaînon entre Bagridés et Clariidés. *Rev. Zool. Bot. Afr.*, 28(3): 369-388.

DE CLERCK N., VAN DYCK D. & A. POSTNOV, 2003. - Non-invasive high-resolution μCT of the inner structure of living animals. *Microsc. Anal.*, 81: 13-15.

DEVAERE S., ADRIAENS D., VERRAES W. & G.G. TEUGELS, 2001. - Cranial morphology of the anguilliform clariid *Channallabes apus* (Günther, 1873) (Teleostei: Siluriformes): Adaptations related to a powerful biting? *J. Zool. Lond.*, 255: 235-250.

DEVAERE S., TEUGELS G.G., ADRIAENS D., HUYSENTRUYT F. & W. VERRAES, 2004. - Redescription of *Dolichallabes microphthalmus* (Poll, 1942) (Siluriformes: Clariidae). *Copeia*, 2004: 108-115.

GREENWOOD P.H., 1961. - A revision of the genus *Dinotopterus* Blgr. (Pisces, Clariidae) with notes on the comparative anatomy of the suprabranchial organs in the Clariidae. *Bull. Br. Mus. Nat. Hist. (Zool.)*, 7: 217-241.

LEVITON AE, GIBBS R.H., HEAL E. & C.E. DAWSON, 1985. - Standards in herpetology and ichthyology: Part I. Standard symbolic code for institutional resource collections in herpetology and ichthyology. *Copeia*, 1985: 802-832.

POLL M., 1942. - Description d'un genre nouveau de Clariidae originaire du Congo belge. *Rev. Zool. Bot. Afr.*, 36: 96-100.

POLL M., 1957. - Redescription du *Gymnallabes tihoni* Poll 1944, Clariidae microphthalme du Stanley-Pool (Congo belge). *Rev. Zool. Bot. Afr.*, 55: 237-248.

POLL M., 1973. - Les yeux des poissons aveugles africains et de *Caecomastacembelus brichardi* Poll, en particulier. *Ann. Spéléo.*, 28: 221-230.

POLL M., 1977. - Les genres nouveaux *Platyallabes* et *Platyclarias* comparés au genre *Gymnallabes* Gthr. Synopsis nouveau des genres de Clariidae. *Bull. Class. Sci.*, 5: 122-149.

POSTNOV A., DE CLERCK N. & D. VAN DYCK, 2002. - 3D invivo X-ray microtomography of living snails. *J. Microsc.*, 205: 201-204.

ROBERTS T.R. & D.J. STEWART, 1976. - An ecological and systematical survey of fishes in the rapids of the lower Zaire or Congo River. *Bull. Mus. Comp. Zool.*, 147: 239-317.

SABAJ M.H., PAGE L.M., LUNDBERG J.G., FERRARIS C.J., ARMBUSTER J.W. Jr., FRIEL J.P. & P.J. MORRIS, 2004. - All Catfish Species Inventory Website. Internet address: http://clade.acnatsci.org/allcatfish.

TEUGELS G.G., 2003. - State of the art of recent siluriform systematics. *In*: Catfishes (Arratia G., Kapoor A.S., Chardon M. & R. Diogo, eds), pp 317-352. Enfield, NH and Plymouth, UK: Science Publishers, Inc.

TEUGELS G.G. & D. ADRIAENS, 2003. - Taxonomy and phylogeny of Clariidae. An overview. *In*: Catfishes (Arratia G., Kapoor A.S., Chardon M. & R. Diogo, eds), pp 465-487. Enfield, NH and Plymouth, UK: Science Publishers, Inc.

TEUGELS G.G., DENAYER B. & M. LEGENDRE, 1990. - A systematic revision of the African catfish genus *Heterobranchus* Geoffroy Saint-Hilaire, 1809 (Pisces, Clariidae). *Zool. J. Linn. Soc.*, 98: 237-257.

TEUGELS G.G., DIEGO R.C., POUYAUD L. & M. LEGENDRE, 1999. - Redescription of *Clarias macrocephalus* (Siluriformes: Clariidae) from South-East Asia. *Cybium*, 23: 285-295.

THIEME M.L., ABELL R.A., STIASSNY M.L.J., LEHNER B., SKELTON P.H., TEUGELS G.G., DINERSTEIN E., KAMDEM-TOHAM A., BURGESS N. & D.M. OLSON, eds, 2004. - Freshwater Ecoregions of Africa: A Conservation Assessment. 431 p. Washington, DC, USA: Island Press.

WEBB J.F., 1989. - Gross morphology and evolution of the mechanoreceptive lateral-line system in teleost fishes. *Brain, Behav. Evol.*, 33: 34-53.